Journal of Constructional Steel Research 105 (2015) 49–59

Contents lists available at ScienceDirect

Journal of Constructional Steel Research

Analytical modeling of rectangular SC wall panels

Siamak Epackachi [a,*], Andrew S. Whittaker [a], Yin Nan Huang [b]

[a] Department of Civil, Structural and Environmental Engineering, University at Buffalo, Buffalo, NY 14260, United States
[b] Department of Civil Engineering, National Taiwan University, Taipei, Taiwan

ARTICLE INFO

Article history:
Received 12 July 2014
Accepted 10 October 2014
Available online xxxx

Keywords:
Steel-plate concrete composite walls
Infill concrete
Steel faceplates
Macro models
Analytical model
Finite element model
LS-DYNA

ABSTRACT

A complete family of seismic analysis and design tools for a structural component or system would include micro-models suitable for finite element analysis of individual components, macro-models suitable for analysis of a framing system, and simplified models suitable for preliminary analysis and design upon which macro-models can later be based.

This paper presents a simplified model for analysis of flexure- and flexure-shear-critical rectangular steel-plate composite (SC) walls. A reliable straightforward method is presented to calculate the monotonic force–displacement response of an SC wall. The proposed analytical model is verified using results of finite element analyses of SC walls with three aspect ratios (= 0.5, 1 and 2), reinforcement ratios ranging from 2% to 5%, wall thicknesses of 254 mm, 508 mm, and 762 mm, and concrete compressive strengths of 27.5 MPa and 48.3 MPa. The results of analysis using the simplified model compares very favorably with those obtained by finite element analysis of validated LS-DYNA models. The accuracy of the proposed method to simulate the monotonic response of multi-story SC walls is investigated.

1. Introduction

Typical steel-plate concrete (SC) composite walls are composed of steel faceplates, infill concrete, headed steel studs anchoring the faceplates to the infill, and tie rods connecting the two faceplates through the infill. Fig. 1 presents a cut-away view of a typical SC wall panel.

The considerable interest in the use of steel-plate concrete (SC) composite shear walls in safety-related nuclear facilities has motivated Japanese, Korean, Canadian and US researchers to investigate the in-plane behavior of SC walls. Much of the early work focused on shear-critical walls, namely, those walls with boundary columns and flanges and those rectangular walls and rectangular walls with low aspect ratios. Takeda et al. [1] proposed a tri-linear curve including the elastic, pre-buckling, and post-buckling regions. Suzuki et al. [2] developed a macro model to predict the peak shearing resistance of H-shaped SC walls using a lower bound theory. A tri-linear shear force-shear strain relationship was proposed by Akita et al. [3] to consider concrete cracking, faceplate yielding, and concrete crushing in SC walls. Emori et al. [4] proposed that the shear resistance of an SC wall be calculated as the sum of the shear strength of the steel faceplates ($0.6A_sf_y$) and 30% of the axial compressive force in the infill concrete (A_cf_c). A tri-linear relationship for in-plane shear was proposed by Ozaki et al [5], which included elastic, post-concrete cracking, and post-faceplate yielding regions; the peak shearing strength was set equal to the yield strength (A_sf_y) of the steel faceplates. Varma et al. [6,7] proposed a tri-linear shear force–shear strain relationship for in-plane shear response with similar break points and peak shearing strength. The above studies focused on behavior in pure shear. Flexure and flexure–shear behaviors have not been studied as thoroughly.

A complete family of seismic analysis and design tools for SC walls should include micro-models suitable for finite element analysis of individual components, macro-models suitable for analysis of a framing system, and simplified models suitable for preliminary analysis and design upon which macro-models can later be based. This paper presents a simplified procedure to predict the flexure and flexure–shear responses of rectangular SC walls using moment–curvature and shearing force–shearing strain relationships. The model is verified using results of finite element analysis of DYNA models that were validated [17] using data from large-scale physical experiments [8–10]. Shear-critical SC walls are not addressed. The notation is summarized in a compact form at the end of the paper and variables are not defined after equations.

2. Simplified monotonic analysis of SC walls

Xu et al. [11] calculated the lateral force–lateral displacement relationship for an RC column assuming concentrated hinging and addressing coupling between axial force, shear force and bending moment. Nonlinear response was simulated using flexural and shear springs at the ends of the column. Backbone curves were established in flexure

* Corresponding author at: Department of Civil, Structural and Environmental Engineering, 212 Ketter Hall, University at Buffalo, The State University of New York, Buffalo, NY 14260, US.
E-mail addresses: siamakep@buffalo.edu (S. Epackachi), awhittak@buffalo.edu (A.S. Whittaker), ynhuang@ntu.edu.tw (Y.N. Huang).

http://dx.doi.org/10.1016/j.jcsr.2014.10.016
0143-974X/

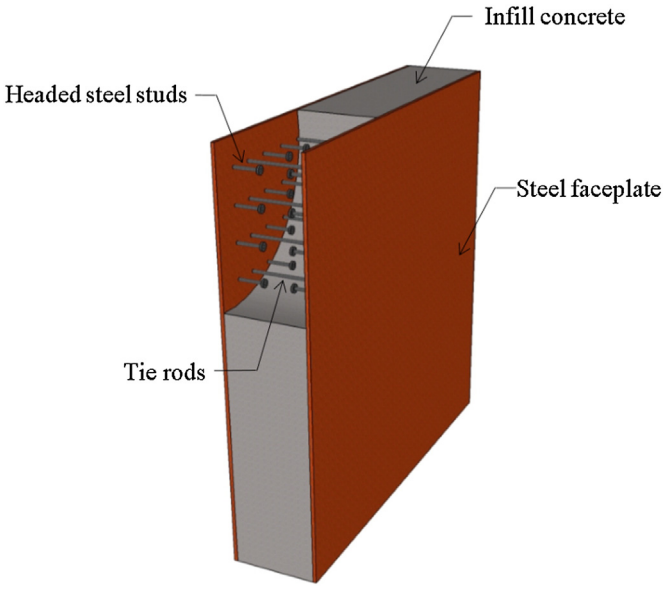

Fig. 1. SC wall panel.

and shear for the nonlinear springs that were assigned to the sub-elements comprising the column. The Modified Compression Field Theory (MCFT), as developed by Vecchio et al. [12], was used to establish the moment–curvature and shearing force–shearing strain relationships for each sub-element. The flexural and shearing deformations at the top of the column, calculated by integrating the curvature and shear strain in each section along the column height, were used to obtain the moment–rotation and shearing force–shearing displacement relationships adopted for flexural and shear springs, respectively.

This approach is used to establish the in-plane flexure–shear response of rectangular SC walls. Fig. 2 illustrates the general procedure.

The in-plane flexure–shear response of an SC wall subjected to lateral loading is calculated in eight steps as follows: 1) discretize the wall element into sub-elements along its height and between the points of application of lateral loading (termed a wall panel), 2) calculate the shear force–shear strain relationship for the panel using the equations included in Table 1, 3) calculate the moment–curvature relationship for the cross-sections of the SC wall panel using the equations included in Table 2, 4) modify the moment–curvature relationships of step 2 to account for flexure–shear interaction in the steel faceplates, 5) set the shearing capacity of the panel (V_t^{max}) to the smaller of a) the peak shearing force calculated in step 2 (V_s^{max}), and b) the shearing force corresponding to the flexural strength calculated in step 4 (V_f^{max}), 6) increment the applied shearing force from zero to the shearing capacity of the SC wall calculated in step 5 and calculate the incremental moment applied to each sub-element for each increment of the shearing force (see Fig. 2), 7) calculate the values of the curvature and shearing strain in each sub-element using the moment–curvature and shearing force–shearing strain relationships calculated in steps 2 and 4, and 8) calculate the flexural (Δ_f), shear (Δ_s) and total (Δ_t) displacements corresponding to each increment of the shearing force as:

$$\Delta_f = \sum_{i=1}^{m} \phi_i \Delta y_i y_i \tag{1}$$

$$\Delta_s = \sum_{i=1}^{m} \gamma_i \Delta y_i = \gamma_i \sum_{i=1}^{m} \Delta y_i = \gamma_i H \tag{2}$$

$$\Delta_t = \Delta_f + \Delta_s. \tag{3}$$

The shearing force–shearing strain and moment–curvature relationships required to make these calculations for an SC wall panel are presented next.

2.1. Shearing force–shearing strain relationship

Fig. 3 presents the shearing force–shearing strain relationship assumed in this study. The coordinates of the three break points (A, B, and C) in the Fig. 3 define the elastic (origin-A), post-concrete cracking (A–B), post-faceplate yielding (B–C) regions of the response. The calculation of these coordinates is discussed below.

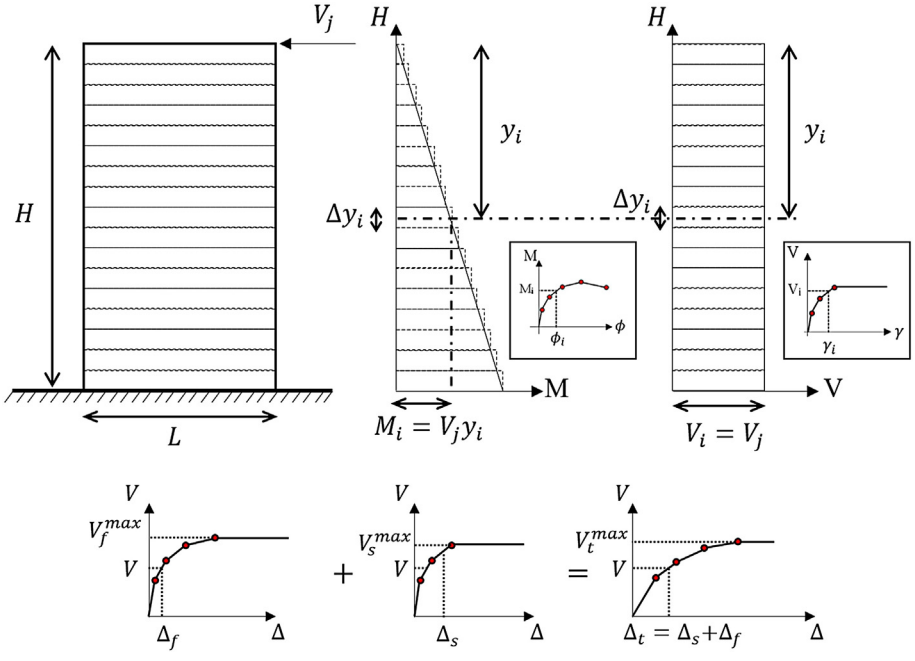

Fig. 2. Simplified monotonic analysis of SC walls.

Table 1
Calculation of the shearing response of an SC wall panel.

Limit state	Shearing force (kN)	Shearing stiffness (kN)
Concrete cracking	$V_{cr} = 0.00017\sqrt{f_c'}(A_c + nA_s)$	$K_e = G_s A_s + G_c A_c$
Yielding of the steel faceplates[1,2]	$V_y = \frac{K_\alpha + K_\beta}{\sqrt{3K_\alpha^2 + K_\beta}} A_s f_y$	$K_{cr} = K_\alpha + K_\beta$
Concrete crushing[3]	$V_u = \frac{1}{2}\left(\sqrt{1 + \left(\frac{H}{L}\right)^2} + (\eta - 1)\frac{H}{L}\right) A_c f_c'$	$K_y = \frac{V_u - V_y}{0.006 - \left(\frac{V_{cr}}{K_e} + \frac{V_y - V_{cr}}{K_{cr}}\right)}$

[1] $K_\alpha = G_s A_s$.
[2] $K_\beta = \frac{1}{\frac{2(1+\nu_s)}{A_s E_s} + \frac{4}{A_c E_c{}^{cr}}}$.
[3] $\eta = A_s f_y / A_c f_c'$.

2.1.1. Concrete cracking: Break point A

In this study, the shear behavior of SC walls developed by Ozaki et al. [5] and Varma et al. [6] is used to simulate the elastic shear response of SC walls. Varma et al. [6] parsed the in-plane response of an SC wall in shear into three regions: 1) elastic, 2) concrete cracking, and 3) steel faceplate yielding. In the elastic range, the infill concrete and steel faceplates are modeled using isotropic elastic and isotropic elastic plane-stress behaviors, respectively. The shearing strength of the SC wall at the onset of concrete cracking is calculated by multiplying the area of the transformed SC wall cross-section by a concrete shear stress equal to $0.00017\sqrt{f_c'}$ MPa. The elastic shear stiffness of the SC wall is calculated as the sum of the shear stiffness of the infill concrete and the steel faceplates. Equations to calculate the coordinates of point A are presented in Table 1.

2.1.2. Steel faceplate yielding: Break point B

After concrete cracking, Ozaki et al. [5] and Varma et al. [6] assumed the infill concrete to behave as an orthotropic elastic material with no stiffness perpendicular to the direction of cracking and 70% of the elastic compression modulus (E_c) in the orthogonal direction. The stiffness of the cracked SC wall is calculated assuming orthotropic behavior of the infill concrete and isotropic elastic plane stress behavior of the steel faceplates. These assumptions are used here to calculate the shearing stiffness of a cracked SC wall prior to faceplate yielding. The shearing force at the onset of faceplate yielding and the shear stiffness of a cracked SC wall are presented in Table 1. The equations are derived in Akita et al. [3] and Hong et al. [13] and are not repeated here.

2.1.3. Concrete crushing: Break point C

Akita et al. [3] estimated the ultimate shear strain for an SC wall in pure shear to be 6000 micro strain on the basis of test data. Tsuda et al. [14] and Hong et al. [13] have used this value to help characterize the response of SC walls in pure shear. The equations for post-yielding stiffness and shearing strength at concrete crushing, which are presented in Table 1, are from Hong et al. [13] and are not repeated here.

2.2. Moment–curvature relationship

The moment–curvature relationship for an SC wall is established at the points of 1) concrete cracking, 2) yielding of the steel faceplates on the tension side of the wall, 3) yielding of the steel faceplates on the compression side of the wall, and 4) maximum concrete compressive strain equal to ε_{c0}: the concrete strain at f_c' [16]. Fig. 4 illustrates the calculations.

Assumptions are made to calculate flexural strength, consistent with the development of a simplified procedure: (1) plane sections remain plane after bending, (2) flexure–shear interaction is considered in the calculation of the stress in the steel faceplates but its effect on the response of the infill concrete is ignored, (3) tensile strength of concrete is ignored, (4) flexural strength of infill concrete is derived using an equivalent rectangular stress-block, (5) the steel faceplates and infill concrete are perfectly bonded, (6) the effects of axial force are ignored, and (7) strain hardening of the faceplates is ignored.

The moment–curvature relationship of the wall cross-section can be represented by the piecewise linear relationship of Fig. 5. The coordinates of points A through E in Fig. 5 can be calculated using equations included in Table 2.

2.3. Concrete behavior

The concrete stress–strain relationship proposed by Tsai [15] is used to describe the behavior of the infill concrete:

$$\frac{f_c}{f_c'} = \frac{n'x}{1 + \left(n' - \frac{r}{r-1}\right)x + \frac{x^r}{r-1}}. \tag{6}$$

Chang et al. [16] proposed Eq. (7) to calculate the concrete strain corresponding to the peak stress, and Eqs. (8) and (9) to establish the shape

Table 2
Calculation of the flexural response of an SC wall panel.

Limit state	$\alpha = \frac{\varepsilon}{L}$	ϕ	M
Concrete cracking	$\alpha_{cr} = \frac{L}{2}$	$\phi_{cr} = \frac{2f_t}{LE_c}$	$M_{cr} = \frac{f_t L}{6}(A_c + nA_s)$
Yielding of the steel faceplates on tension side of the wall[1]	$\alpha_y^t = \frac{\sqrt{\rho'}}{\sqrt{\rho'+1}+\sqrt{\rho'}}$ $L_y^t = L\left(\frac{2\alpha^3 - 3\alpha^2 - \rho'}{12\rho'(\alpha-1)}\right)$	$\phi_y^t = \frac{\varepsilon_y}{L(1-\alpha)}$	$M_y^t = A_s f_y^e L_y^t$
Yielding of the steel faceplates on compression side of the wall[2]	$\alpha_y^c = \frac{1}{\gamma+2}$ $L_c' = \alpha L\left(\frac{1-\beta_2\alpha}{2}\right), L_s' = \alpha L(1 - \frac{4}{3}\alpha)$	$\phi_y^c = \frac{\varepsilon_y}{L\alpha}$	$M_y^c = \beta_1\beta_2 f_c' A_c L_c' + A_s f_y^e L_s'$
Maximum concrete compressive strain equals to ε_{c0}	$\alpha_u = \frac{1}{\gamma+2}$ $L_c'' = \alpha L\left(\frac{1-\beta_2\alpha}{2}\right), L_s'' = \alpha L\left(1 - \alpha - \frac{\alpha k^2}{3}\right)$	$\phi_u = \frac{\varepsilon_{c0}}{L\alpha}$	$M_u = \beta_1\beta_2 f_c' A_c L_c'' + A_s f_y^e L_s''$

[1] $\rho' = \frac{2t_s n}{t_c}$.
[2] $\gamma = \frac{n\beta_1\beta_2 f_c'}{\rho' f_y}$.

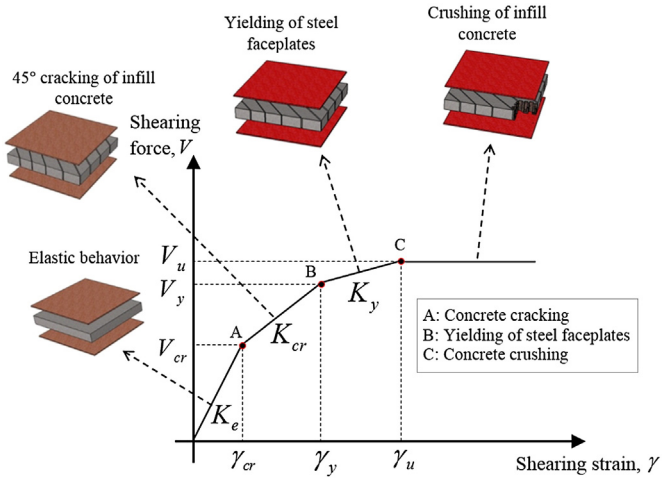

Fig. 3. In-plane shear response of SC walls.

of the stress–strain relationship:

$$\varepsilon_{c0} = \frac{(f'_c)^{1/4}}{728} \tag{7}$$

$$n' = \frac{}{(f'_c)^{3/8}} \tag{8}$$

$$r = \frac{f'_c}{5.2} - 1.9. \tag{9}$$

Fig. 6 presents the stress–strain relationships for unconfined uniaxial compressive strengths between 20.6 and 48.3 MPa, which is considered a practical range for infill concrete in SC walls, noting that the strain limit for calculations is ε_{c0}.

Fig. 4 presents that the calculation of the equivalent rectangular stress block parameters is required for the calculations of flexural strengths corresponding to two limit states: 1) yielding of the steel faceplates on the compression side of the wall, and 2) maximum concrete compressive strain equal to ε_{c0}. The values of β_1 and β_2 corresponding to these limit states, presented in Table 3, are calculated [17] assuming that the equivalent rectangular stress bock recovers the area under the stress–strain relationship and the location of its resultant. Values of the two stress block parameters are presented for $20.6 \le f'_c \le$

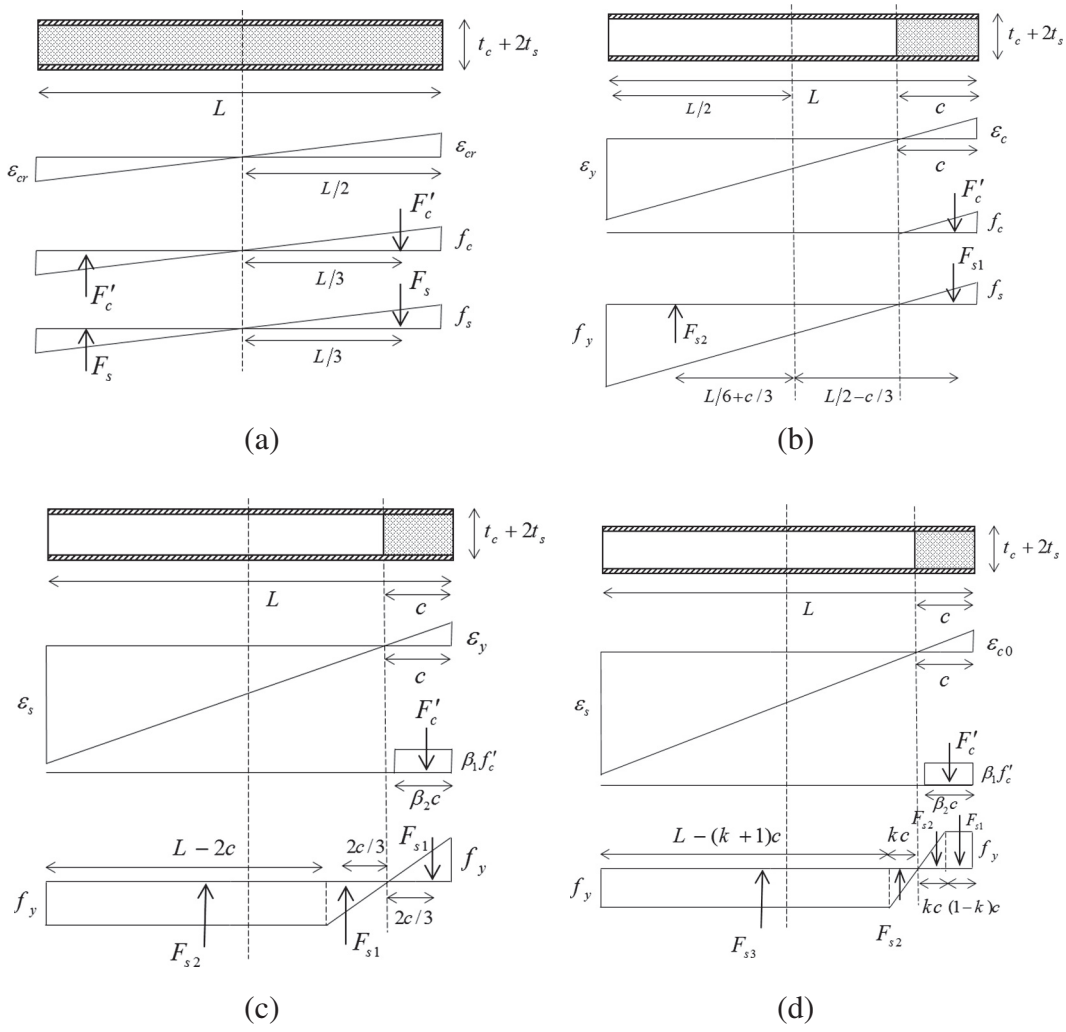

Fig. 4. Moment–curvature calculation. (a) Concrete cracking. (b) Steel faceplate yielding on tension side of the wall. (c) Steel faceplate yielding on compression side of the wall. (d) Maximum concrete compressive strain equals to strain corresponding to f'_c.

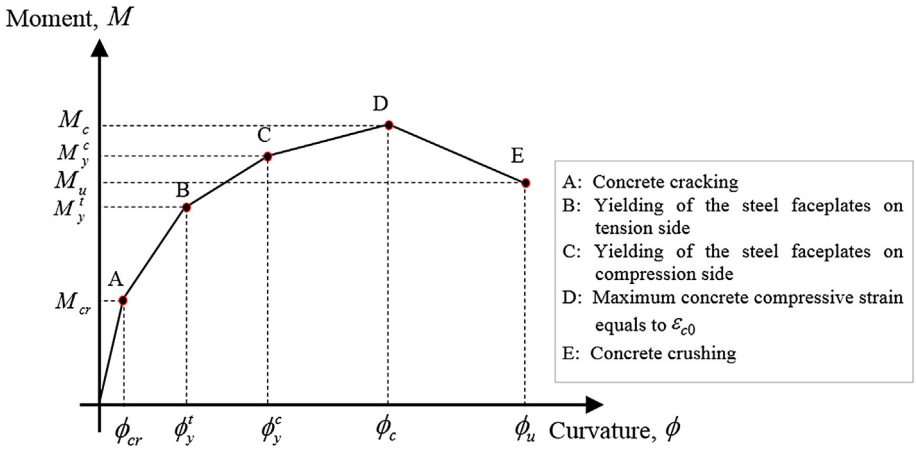

Fig. 5. Moment–curvature relationship of SC wall.

48.3 MPa and faceplate yield strengths of 250, 310 and 415 MPa. Values for other combinations of f_c' and f_y can be interpolated.

2.4. Steel material

Consistent with the development of a simplified procedure, the flexural strength of the faceplates is calculated assuming a steel stress, f_y', equal to the average of the yield and tensile strengths of the steel faceplates.

2.5. Flexure–shear interaction in the steel faceplates

The effect of shearing force on the moment–curvature relationship is considered by reducing the yield stress of the steel faceplates. The effect of flexure–shear interaction on the response of the infill concrete is ignored. An effective yield stress is calculated as

$$f_y^e = \sqrt{f_y'^2 - 3\tau^2} \tag{10}$$

which is based on the Von-Mises yield condition and assumes zero horizontal stress along the length of the steel faceplates. The equivalent shear stress in the steel faceplates, τ in Eq. (10), is calculated by dividing the shearing force associated with the flexural resistance of the steel faceplates by the cross-section area of the faceplates. Substituting $\tau = f_y' L_s''/(M/V)$ into Eq. (10)

$$f_y^e = f_y'\left(\sqrt{1-\zeta^2}\right) \tag{11}$$

where ζ is

$$\zeta = \sqrt{3}\left(\frac{3\gamma + 3 - k^2}{3(\gamma+2)^2}\right)\left(\frac{VL}{M}\right) \le 1 \tag{12}$$

and γ is calculated using equation included in Table 2. The effective yield stress of the steel faceplates is a function of the concrete uniaxial compressive strength, the yield stress of the steel faceplates, the reinforcement ratio, and the normalized moment-to-shear ratio (M/VL). Note the normalized moment-to-shear ratio is identical to the wall aspect ratio, H/L), for a single story wall panel of height H and length L. The influence of the normalized moment-to-shear ratio and concrete strength on f_y^e is presented in Fig. 7. Results in Fig. 7 are presented for a wall panel with 1524 mm length, 254 mm thickness, and 6.4 mm-thick steel faceplates with 250 MPa yield strength. Fig. 7 indicates that a) the

Table 3
Values of the stress block parameters.

f_c' (MPa)	Steel faceplate yielding on compression side of the wall						Maximum concrete compressive strain equal to ε_{c0}	
	f_y = 250 MPa		f_y = 310 MPa		f_y = 415 MPa			
	β_1	β_2	β_1	β_2	β_1	β_2	β_1	β_2
20.6	0.77	0.73	0.83	0.74	0.92	0.78	0.91	0.77
27.5	0.68	0.71	0.75	0.72	0.88	0.75	0.88	0.75
34.5	0.62	0.70	0.69	0.71	0.84	0.73	0.87	0.74
41.5	0.57	0.70	0.64	0.70	0.80	0.72	0.86	0.73
48.3	0.54	0.69	0.61	0.70	0.76	0.71	0.83	0.72

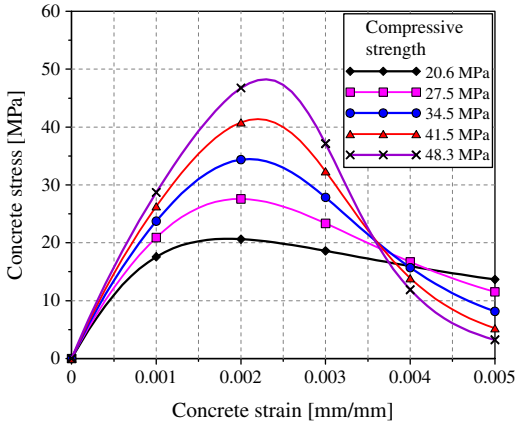

Fig. 6. Unconfined uniaxial compressive stress–strain relationships for infill concrete.

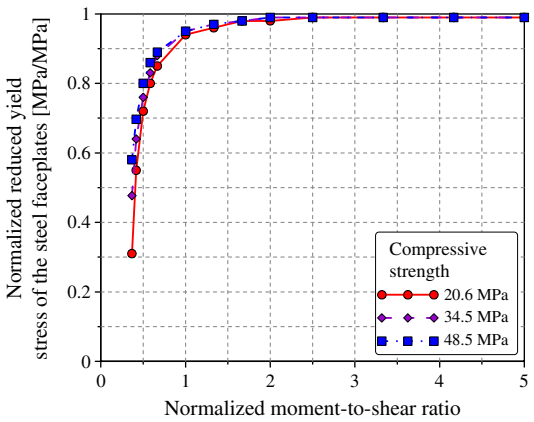

Fig. 7. Effective yield stress of the steel faceplates.

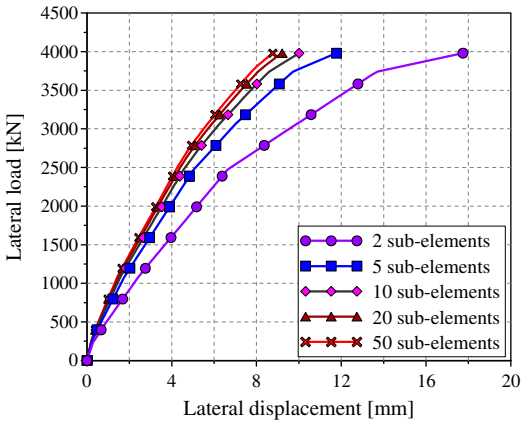

Fig. 8. Force–displacement relationships of SC walls with differing numbers of sub-elements.

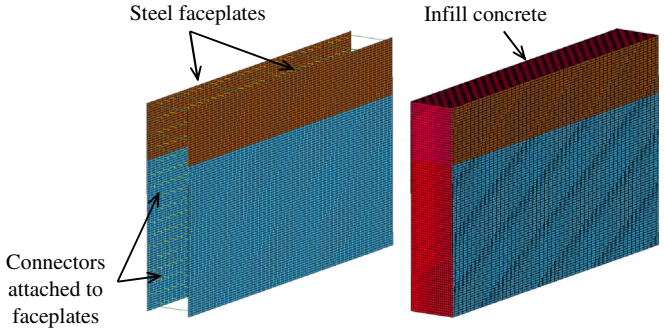

Fig. 9. LS-DYNA model.

yield stress is significantly reduced for aspect ratio less than one on account of flexure–shear interaction, and b) the reduction in yield stress diminishes with increasing concrete compressive strength because flexure–shear interaction decreases with an increase in the shearing load resisted by the infill concrete.

2.6. Vertical discretization

The vertical discretization of an SC wall panel will affect the calculation of response because the effects of flexure–shear interaction change continuously. Results are presented in Fig. 8 for a wall panel with an aspect ratio of 1.0, 3810 mm length, 254 mm thickness, and 4.8 mm-thick steel faceplates of 250 MPa yield strength. The results of Fig. 8 and those presented in Epackachi [17] for other aspect ratios, indicate that 10 elements between points of application of lateral load are sufficient.

2.7. Validation of the simplified monotonic analysis

The simplified monotonic analysis procedure is validated using results of finite element analysis of 36 rectangular SC walls performed using LS-DYNA [18,19]. The four design variables considered are 1) aspect ratio (0.5, 1.0 and 2.0), 2) reinforcement ratio (2% to 5%), 3) wall thickness (254, 508 and 762 mm), and 4) compressive strength of infill concrete (27.5 MPa and 48.3 MPa). Validation of the baseline model

Table 4
Properties of the DYNA models.

No.	SC wall type	Model	Concrete strength (MPa)	Aspect ratio	$H \times L \times T$ (mm × mm × mm)	t_s (mm)	Reinforcement ratio (%)
1	Low-aspect ratio SC walls	LAN254-4	27.5	0.5	1905 × 3810 × 254	4.8	3.8
2		LAI254-4	48.3	0.5	1905 × 3810 × 254	4.8	3.8
3		LAN254-5	27.5	0.5	1905 × 3810 × 254	6.4	5.0
4		LAI254-5	48.3	0.5	1905 × 3810 × 254	6.4	5.0
5		LAN508-4	27.5	0.5	1905 × 3810 × 508	4.8	1.9
6		LAI508-4	48.3	0.5	1905 × 3810 × 508	4.8	1.9
7		LAN508-5	27.5	0.5	1905 × 3810 × 508	12.7	5.0
8		LAI508-5	48.3	0.5	1905 × 3810 × 508	12.7	5.0
9		LAN762-4	27.5	0.5	1905 × 3810 × 762	7.9	2.1
10		LAI762-4	48.3	0.5	1905 × 3810 × 762	7.9	2.1
11		LAN762-5	27.5	0.5	1905 × 3810 × 762	19.1	5.0
12		LAI762-5	48.3	0.5	1905 × 3810 × 762	19.1	5.0
13	Intermediate-aspect ratio SC walls	IAN254-4	27.5	1.0	3810 × 3810 × 254	4.8	3.8
14		IAI254-4	48.3	1.0	3810 × 3810 × 254	4.8	3.8
15		IAN254-5	27.5	1.0	3810 × 3810 × 254	6.4	5.0
16		IAI254-5	48.3	1.0	3810 × 3810 × 254	6.4	5.0
17		IAN508-4	27.5	1.0	3810 × 3810 × 508	4.8	1.9
18		IAI508-4	48.3	1.0	3810 × 3810 × 508	4.8	1.9
19		IAN508-5	27.5	1.0	3810 × 3810 × 508	12.7	5.0
20		IAI508-5	48.3	1.0	3810 × 3810 × 508	12.7	5.0
21		IAN762-4	27.5	1.0	3810 × 3810 × 762	7.9	2.1
22		IAI762-4	48.3	1.0	3810 × 3810 × 762	7.9	2.1
23		IAN762-5	27.5	1.0	3810 × 3810 × 762	19.1	5.0
24		IAI762-5	48.3	1.0	3810 × 3810 × 762	19.1	5.0
25	High-aspect ratio SC walls	HAN254-4	27.5	2.0	7620 × 3810 × 254	4.8	3.8
26		HAI254-4	48.3	2.0	7620 × 3810 × 254	4.8	3.8
27		HAN254-5	27.5	2.0	7620 × 3810 × 254	6.4	5.0
28		HAI254-5	48.3	2.0	7620 × 3810 × 254	6.4	5.0
29		HAN508-4	27.5	2.0	7620 × 3810 × 508	4.8	1.9
30		HAI508-4	48.3	2.0	7620 × 3810 × 508	4.8	1.9
31		HAN508-5	27.5	2.0	7620 × 3810 × 508	12.7	5.0
32		HAI508-5	48.3	2.0	7620 × 3810 × 508	12.7	5.0
33		HAN762-4	27.5	2.0	7620 × 3810 × 762	7.9	2.1
34		HAI762-4	48.3	2.0	7620 × 3810 × 762	7.9	2.1
35		HAN762-5	27.5	2.0	7620 × 3810 × 762	19.1	5.0
36		HAI762-5	48.3	2.0	7620 × 3810 × 762	19.1	5.0

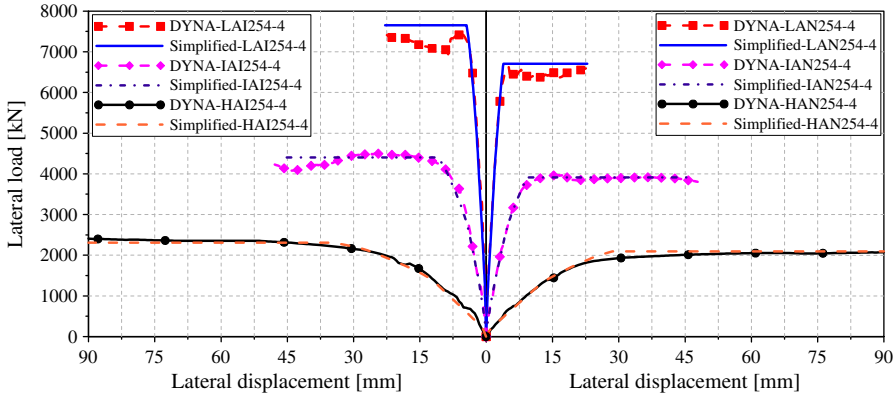

Fig. 10. Force–displacement relationship for 254 mm thick walls with 3.8% reinforcement ratio.

was performed by simulation of the nonlinear cyclic in-plane behavior of four large-scale rectangular SC walls tested at the University at Buffalo [8].

Table 4 summarizes the design parameters for each analysis case. Each entry is identified using aspect ratio wall (L for low-aspect ratio, 0.5; I for intermediate-aspect ratio, 1.0; and H for high-aspect ratio, 2.0); concrete compressive strength (N for normal-strength concrete and I for intermediate-strength concrete); the thickness; and reinforcement ratio. For example, LAN254-4 represents a 254 mm thick low-aspect ratio ($H/L = 0.5$) SC wall with normal-strength concrete ($f'_c = 27.5$ MPa) and 4% reinforcement ratio ($2t_s/t_c = 0.04$).

The wall length in all the DYNA models is 3810 mm. The spacing of the studs and tie rods are 127 mm and 508 mm, respectively. The diameter of the studs and tie rods is 9.6 mm. The values of the spacing and the diameter of the studs and tie rods are selected based on the specifications proposed by AISC N690s1 [20]. The smeared crack Winfrith model (MAT085) in LS-DYNA, developed by Broadhouse [21], is used to model the infill concrete. The Broadhouse model provides information on the orientation of the cracking planes (up to three orthogonal cracks for each element) and the width of the cracks [22]. The plastic-damage model, Mat-Plasticity-With-Damage (MAT081) in LS-DYNA [19], is used for the steel faceplates and connectors. The nominal yield and ultimate strengths of the studs and tie rods are assumed to be 345 and 517 MPa, respectively. ASTM A36 steel is assumed for the steel faceplates, with values of yield stress and tensile strength of 262 and 380 MPa, respectively. Friction between the infill concrete and the steel faceplates is considered. The studs and tie rods are coupled to the infill concrete elements. Beam elements are used

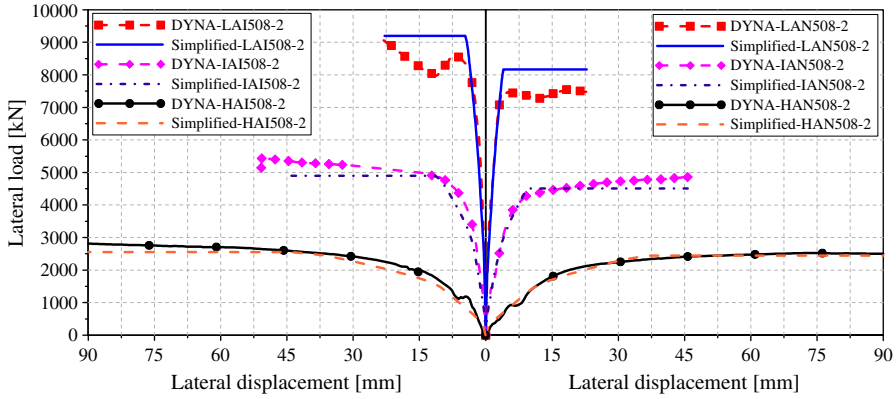

Fig. 11. Force–displacement relationship for 508 mm thick walls with 1.9% reinforcement ratio.

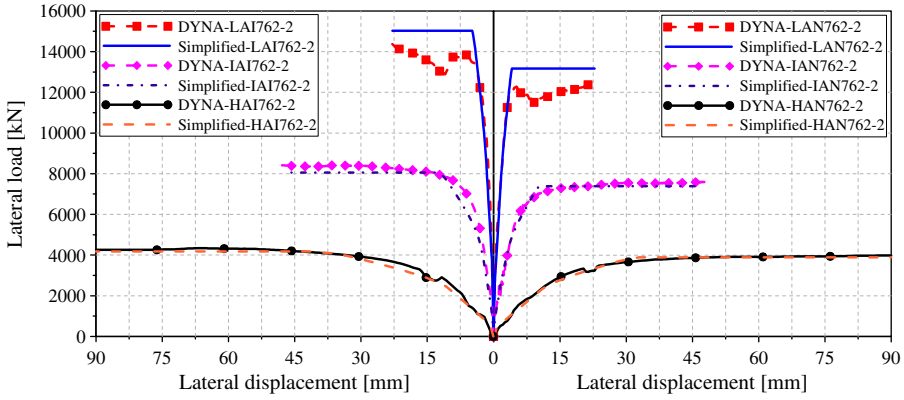

Fig. 12. Force–displacement relationship for 762 mm thick walls with 2.1% reinforcement ratio.

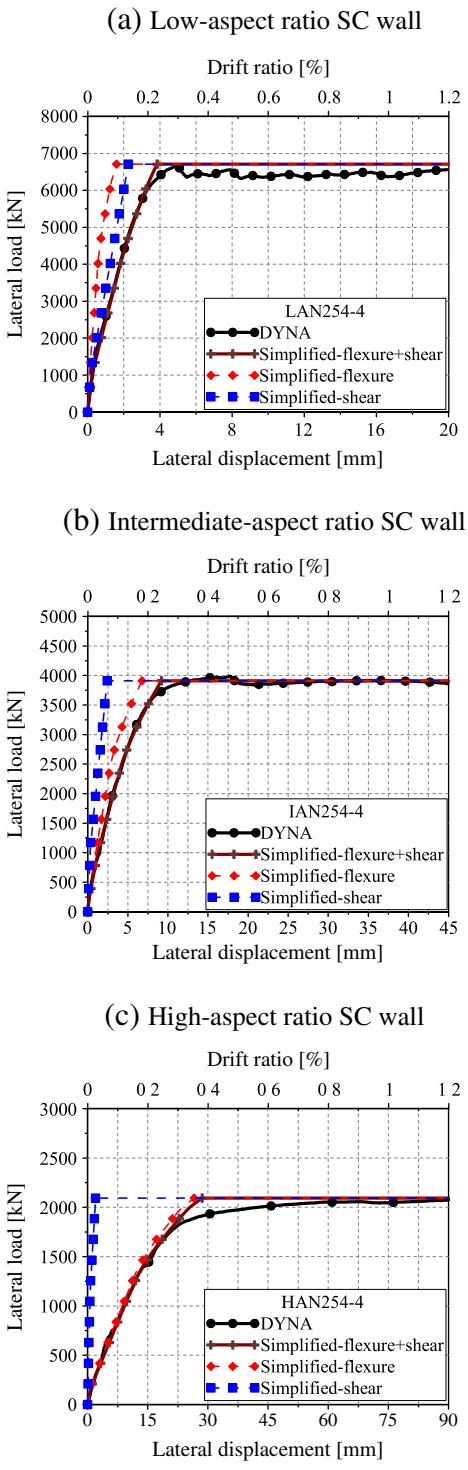

Fig. 13. Analytically- and DYNA-predicted force–displacement relationships for 254 mm thick wall with 3.8% reinforcement ratio. (a) Low-aspect ratio SC wall. (b) Intermediate-aspect ratio SC wall. (c) High-aspect ratio SC wall.

to represent the studs and tie rods. Eight-node solid elements are used to model the infill concrete, and four-node shell elements are used for the steel faceplates. The infill concrete is modeled with 25.4 mm × 25.4 mm × 25.4 mm elements and the steel faceplates are modeled with 25.4 mm × 25.4 mm elements. The connection of the wall to the foundation is assumed to be rigid. The LS-DYNA model is presented in Fig. 9.

Figs. 10–12 present DYNA-predicted shearing force–displacement relationships together with those predicted using the proposed method calculated using 75 sub-elements over the height of the wall panel. Results for other wall panels are presented in Epackachi [17]. The proposed method accurately predicts the monotonic in-plane response of the SC walls with different aspect ratios, reinforcement ratios, concrete strengths, and wall thicknesses up to the point of maximum shear resistance. The peak shearing resistance of the low-aspect ratio walls is slightly over-estimated.

Fig. 13 presents the components of displacement for the analytically derived and DYNA-predicted force–displacement relationships for 254 mm thick rectangular SC walls with a reinforcement ratio of 3.8%. The shearing displacements dominate for an aspect ratio of 0.5 and the flexural displacements dominate for aspect ratios greater than 1.0, which are expected outcomes. The lateral displacement corresponding to shearing strength is underestimated because the stiffness reduction due to the out-of-plane buckling of the steel faceplates has not been considered in the simplified approach but is captured in the DYNA analysis. These results further confirm the utility of the proposed simplified method for monotonic analysis of rectangular SC wall panels.

2.8. Force–displacement response of multi-story SC walls

Single story walls are rarely used in practice and so a simplified method must be appropriate for analysis of multi-story SC walls. Small-size walls are analyzed here to take advantage of prior work and minimize the computational expense. Two three-story walls are analyzed using the proposed method (see Section 2) in MATLAB and the finite element method using DYNA, with the same material models, elements, and boundary conditions used for the analysis of 36 rectangular SC walls. The length and height of the walls are 1524 mm and 3045 mm, respectively. The thickness of the walls is 305 mm; the thickness of each steel faceplate is 4.8 mm. Beams and columns are not included in the models. The SC walls are subjected to uniform and triangular distributions of lateral loads as shown in Fig. 14.

The shear force–shear strain relationship for each panel of the three-story walls (P1, P2, and P3 presented in Fig. 14) was calculated using the equations of Table 1. The moment–curvature relationship for each panel was calculated using an effective yield stress (Eq. (11)) that is a function of the moment-to-shear ratio (M/VL), which depends on the vertical distribution of lateral loads above the panel.

The moment-to-shear ratio for P1 in both SC walls is presented below to illustrate the calculation. The level of the resultant of the lateral loads applied above P1 for the SC walls subjected to uniform and triangular distributions of lateral loads can be calculated using Eqs. (13) and (14), respectively:

$$h_r = \frac{F \times 3H + F \times 2H + F \times H}{F + F + F} = 2H \tag{13}$$

$$h_r = \frac{F \times 3H + 0.67F \times 2H + 0.33F \times H}{F + 0.67F + 0.33F} = 2.34H. \tag{14}$$

The moment-to-shear ratio for P1 is calculated as $h_r/L = 1.33$ ($2H/L$) and $= 1.56$ ($2.34H/L$) for the SC walls subjected to uniform and triangular distributions of lateral loads, respectively.

The flexural displacement at the top of each 1015-mm tall panel was calculated using Eq. (1) with y_i as the distance between the center of ith sub-element of the panel and top of the three-story SC wall. Seventy-five sub-elements were used for each of the three panels. The shear displacement at top of each panel was calculated using Eq. (2). The total displacement at the top of the wall is calculated as:

$$\Delta_t = \left(\Delta_{s1} + \Delta_{f1}\right) + \left(\Delta_{s2} + \Delta_{f2}\right) + \left(\Delta_{s3} + \Delta_{f3}\right). \tag{15}$$

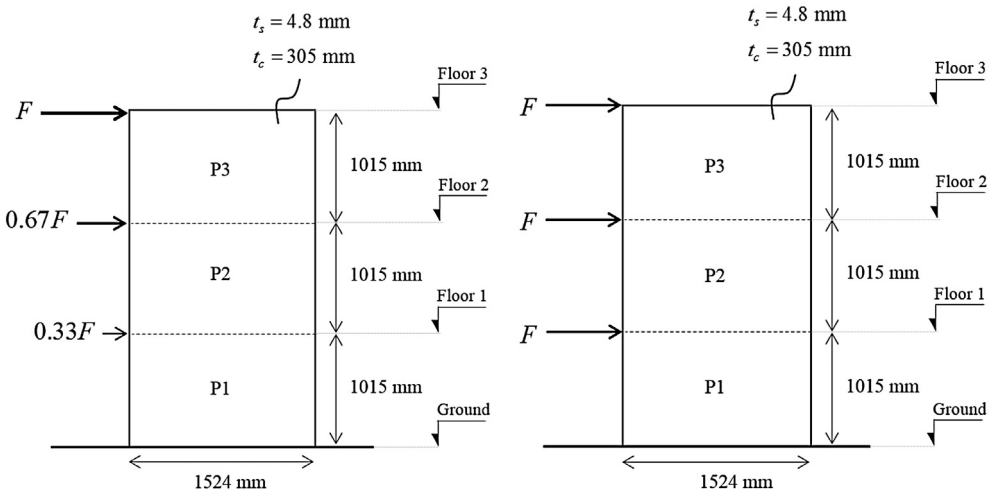

Fig. 14. Elevation view of three-story SC walls subjected to uniform and triangular distributions of lateral loads.

The rotation at the top of each wall panel is calculated as:

$$\theta_j = \theta_{j-1} + \sum_{i=1}^{m} \phi_i^j \Delta y_i^j \tag{16}$$

where i and j denote the sub-element and story numbers, respectively, and $\theta_0 = 0$. The displacement components and rotations at the tops of the panels are defined in Fig. 15.

Responses per Eq. (15) are presented in Fig. 16. The proposed method reasonably predicts the monotonic responses of this three-story SC walls. The initial stiffness is accurately predicted and the peak shearing strength is estimated with less than 10% error.

3. Conclusions

An analytical model for calculating the monotonic response of SC wall panels is developed and verified for the preliminary analysis and design of structures including these walls. The simplified analytical model is verified using the results of DYNA analysis of low, intermediate and high aspect ratio walls, with materials and properties typical of those used in the building and nuclear industries. Flexure and flexure–shear critical walls are considered. The baseline DYNA model was validated using results of large-scale cyclic tests of SC walls with an aspect ratio of 1.0.

The key components of the analytical model for monotonic analysis of rectangular SC walls are a) moment–curvature, and b) shearing force–shearing strain relationships for each wall panel. A step-by-step procedure is presented to calculate response under monotonic loading, which could be coded into MATLAB for design-office applications. Assumptions are made, which are consistent with simplified models and the intended use, including a) axial load effects are ignored, and b) perfect bond between the faceplates and the infill concrete (preventing buckling of the faceplates). The accuracy of the predicted responses of single-story SC panels and a three-story SC wall is

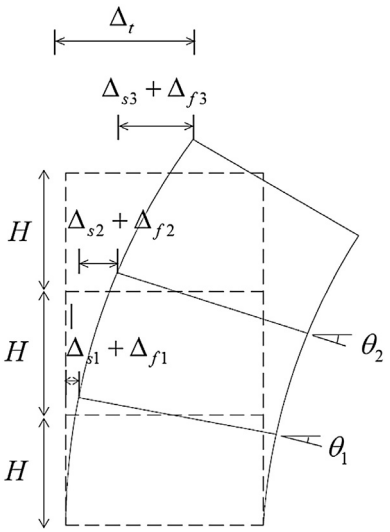

Fig. 15. Displacement calculation in three-story SC wall.

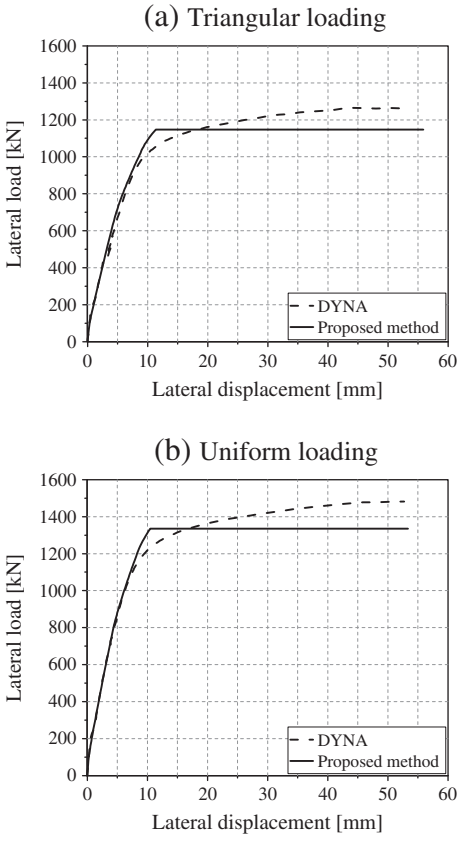

Fig. 16. Analytically- and numerically-predicted responses of three-story SC walls. (a) Triangular loading. (b) Uniform loading.

investigated using the results of DYNA analysis. Good agreement is obtained between the analytical and numerical results.

Notation

A_c Cross-section area of infill concrete
A_s Cross-section area of steel faceplates
c Depth to the neutral axis
E_c Elastic modulus of concrete (MPa)
E_s Elastic modulus of steel (MPa)
$E_c{}^{cr}$ Elastic modulus of cracked concrete $=0.7E_c$
F_c' Compressive force on infill concrete
F_s Compressive and tensile forces in steel faceplates
f_c Concrete stress
f_s Steel stress
f_c' Uniaxial compressive stress of concrete (MPa)
f_y Yield stress of steel faceplates (MPa)
f_u Ultimate stress of steel faceplates (MPa)
f_y^e Effective yield stress of steel faceplates (MPa)
f_y' Average of yield and ultimate stress of steel (MPa)
f_r Modulus of rupture of concrete (MPa)
G_c Elastic shear modulus of concrete (MPa)
G_s Elastic shear modulus of steel (MPa)
H Height of wall panel
h_r Level of the resultant of the lateral loads applied above an SC panel in multi-story SC walls
k Ratio of the yield strain of the steel faceplates to the concrete strain corresponding to the peak stress
K_e Elastic shear stiffness of SC wall
K_{cr} Shear stiffness of SC wall after concrete cracking
K_{cr} Shear stiffness of SC wall after yielding of steel faceplates
K_α Shear stiffness of steel faceplates
K_β Shear stiffness of diagonally cracked infill concrete
L Length of wall
M Bending moment applied on SC wall cross-section
M_i Bending moment in i^{th} sub element
M_{cr} Flexural strength of SC wall at concrete cracking
$M_y{}^t$ Flexural strength of SC wall at yielding of steel faceplates on tension side of the wall
$M_y{}^c$ Flexural strength of SC wall at yielding of steel faceplates on compression side of the wall
M_c Flexural strength of SC wall at maximum concrete compressive strain equal to ε_{c0}
M_u Flexural strength of SC wall at concrete crushing
m Number of sub elements along the height of panel
n Modular ratio
n' Coefficient of concrete stress–strain relationship
r Coefficient of concrete stress–strain relationship
t_c Thickness of infill concrete
t_s Thickness of each steel faceplate
V Shearing force applied on SC wall cross-section
V_{cr} Shearing strength of SC wall at concrete cracking
V_y Shearing strength of SC wall at yielding of the steel faceplates
V_u Shearing strength of SC wall at concrete crushing
V_{ni} In-plane shearing strength of SC wall specified by AISC N690s1
V_i Shearing force in ith sub element
x Ratio of the concrete strain to strain corresponding to peak stress
y_i Distance between the center of ith sub element and top of the wall
Δy_i Height of i^{th} sub element
Δ_{fj} Flexural displacement at top of j^{th} panel
Δ_{sj} Shear displacement at top of j^{th} panel
Δ_t Total displacement at top of SC wall
γ_i Shear strain in i^{th} sub element
γ_{cr} Shear strain of SC wall at concrete cracking
γ_y Shear strain of SC wall at yielding of the steel faceplates
γ_u Shear strain of SC wall at concrete crushing
τ Average shear stress in steel faceplates
ν_s Poisson's ratio for steel
η Strength-adjusted reinforcement ratio
ρ Reinforcement ratio
$\overline{\rho}$ Strength-adjusted reinforcement ratio
ρ' Modulus-adjusted reinforcement ratio
λ Aspect ratio of SC wall
ε_{cr} Concrete cracking strain
ε_c Concrete strain
ε_s Steel strain
ε_{c0} Strain at peak stress of concrete
ε_{sh} Steel strain at hardening
ε_y Steel strain at yielding
α Ratio of neutral axis depth to length of the wall
ϕ_{cr} Curvature of SC wall cross-section at concrete cracking
$\phi_y{}^t$ Curvature of SC wall cross-section at yielding of steel faceplates on tension side of wall
$\phi_y{}^c$ Curvature of SC wall cross-section at yielding of steel faceplates on compression side of wall
ϕ_c Curvature of SC wall cross-section at maximum concrete compressive strain equals to ε_{c0}
ϕ_u Curvature of SC wall cross-section at concrete crushing
ϕ_i Curvature in i^{th} sub-element
β_1 Stress block coefficient
β_2 Stress block coefficient

Acknowledgments

This project was supported in part by the US National Science Foundation under Grant No. CMMI-0829978. This support is gratefully acknowledged.

References

[1] Takeda T, Yamaguchi T, Nakayama T, Akiyama K, Kato Y. Experimental study on shear characteristics of concrete filled steel plate wall. International Association for Structural Mechanics in Reactor Technology (IASMiRT). Raleigh, NC: North Carolina State University; 1995 3–14.
[2] Suzuki N, Akiyama H, Narikawa M, Hara K, Takeuchi M, Matsuo I. Study on a concrete filled steel structure for nuclear power plants (part #4): analytical method to estimate shear strength. International Association for Structural Mechanics in Reactor Technology (IASMiRT). Raleigh, NC: North Carolina State University; 1995 33–8.
[3] Akita S, Ozaki M, Niwa N, Matsuo I, Hara K. Study on steel plate reinforced concrete bearing wall for nuclear power plants (part #2). analytical method to evaluate response of SC walls. International Association for Structural Mechanics in Reactor Technology (IASMiRT). Raleigh, NC: North Carolina State University; 2001.
[4] Emori K. Compressive and shear strength of concrete filled steel box wall. Steel Struct (Korean J) 2002;2:29–40.
[5] Ozaki M, Akita S, Osuga H, Nakayama T, Adachi N. Study on steel plate reinforced concrete panels subjected to cyclic in-plane shear. Nucl Eng Des 2004;228:225–44.
[6] Varma AH, Zhang K, Chi H, Booth PN, Baker T. In-plane shear behavior of SC composite walls: theory vs. experiment. International Association for Structural Mechanics in Reactor Technology (IASMiRT). Raleigh, NC: North Carolina State University; 2011.
[7] Varma AH, Malushte S, Sener K, Lai Z. Steel-plate composite (SC) walls for safety related nuclear facilities: design for in-plane force and out-of-plane moments. Nucl Eng Des 2013;269.
[8] Epackachi S, Nguyen NH, Kurt EG, Whittaker AS, Varma AH. In-plane seismic behavior of rectangular steel-plate composite wall piers. J Struct Eng 2014. http://dx.doi.org/10.1061/(ASCE)ST.1943-541X.0001148.
[9] Epackachi S, Nguyen NH, Kurt EG, Whittaker AS, Varma AH. Numerical and experimental investigation of the in-plane behavior of rectangular steel-plate composite walls. Structures Congress 2014. Boston, Massachusetts, United States: American Society of Civil Engineers; 2014. p. 2478–87.
[10] Epackachi S, Nguyen NH, Kurt EG, Whittaker AS, Varma AH. An experimental study of the in-plane response of steel-concrete composite walls. Structural Mechanics in Reactor Technology Conference (SMiRT-22), San Francisco, California, USA; 2013.
[11] Xu S-Y, Zhang J. Hysteretic shear–flexure interaction model of reinforced concrete columns for seismic response assessment of bridges. Earthq Eng Struct Dyn 2011; 40:315–37.

[12] Vecchio FJ, Collins MP. Modified compression-field theory for reinforced concrete elements subjected to shear. J Am Concr Inst 1986;83:219–31.
[13] Hong SG, Lee SJ, Lee MJ. Steel plate concrete walls for containment structures in Korea: in-plane shear behavior. Infrastruct Syst Nucl Energy 2014:237–57.
[14] Tsuda K, Tatsuo N, Eto H, Akiayama K, Shimizu A, Tanouchi K, et al. Experimental study on steel plate reinforced concrete shear walls with joint bars. International Association for Structural Mechanics in Reactor Technology (IASMiRT). Raleigh, NC: North Carolina State University; 2001.
[15] Tsai WT. Uniaxial compressional stress–strain relation of concrete. J Struct Eng 1988; 114:2133–6.
[16] Chang GA, Mander JB. Seismic energy based fatigue damage analysis of bridge columns: part I-evaluation of seismic capacity. Report No. NCEER-94-0006. Buffalo, NY: National Center for Eartquake Engineeirng Research; 1994.
[17] Epackachi S. Analytical, numerical, and experimental studies on steel-plate concrete (SC) composite walls. Department of Civil, Structural and Environmental Engineering. Buffalo, NY: University at Buffalo; 2014.
[18] LS-DYNA keyword user's manual, volume I. Version 971 R6.0.0, Livermore, CA, USA; 2012.
[19] LS-DYNA keyword user's manual, volume II. Version 971 R6.0.0, Livermore, CA, USA; 2012.
[20] AISC. Specification for design of steel-plate composite (SC) walls in safety-related structures for nuclear facilities. AISC Proposal APPENDIX N9, Chicago, IL; 2013.
[21] Broadhouse BJ. DRASTIC—A compute code for dynamic analysis of stress transients in reinforced concrete. Safety and Engineering Science Devision,AEE, Winfrith, AEEW – R2124; 1986.
[22] Schwer L. The Winfrith concrete model: beauty or beast? Insights into the Winfrith concrete model; 2011.